Chapter 23
Effectiveness of Polypropylene Fibers on Impact and Shrinkage Cracking Behavior of Adobe Mixes

Gerardo Araya-Letelier, Federico C. Antico, Jose Concha-Riedel, Andres Glade and María J. Wiener

23.1 Introduction

The earthen construction materials are characterized by their wide range of applications, availability, recyclability, thermal inertia, acoustic performance, and lower cost and environmental impacts compared to industrialized materials such as fired clay bricks (Cataldo-Born et al. 2016; Donkor and Obonyo 2015; Millogo et al. 2014; Minke 2000, 2006).

Although the widespread use and advantages of earthen materials, their performance is reduced compared to industrialized construction materials in terms of tensile and flexural strength, toughness, fracture toughness, water erosion resistance, and drying shrinkage cracking (Avrami et al. 2008; Minke 2000, 2006). To lessen some of these shortcomings, earthen materials can be reinforced with the incorporation of natural fibers such as straw, sisal, and wool (Aymerich et al. 2012; Galan-Marin et al.

G. Araya-Letelier (✉)
Pontificia Universidad Católica de Chile, Santiago, Chile
e-mail: gerardo.araya@uc.cl

F. C. Antico · A. Glade
Universidad Adolfo Ibáñez, Viña del Mar, Chile
e-mail: federico.antico@uai.cl

A. Glade
e-mail: aglade@alumnos.uai.cl

J. Concha-Riedel
Universidad Adolfo Ibáñez, Santiago, Chile
e-mail: jose.concha@uai.cl

M. J. Wiener
Purdue University, West Lafayette, USA
e-mail: wiener@purdue.edu

B. V. V. Reddy et al. (eds.), *Earthen Dwellings and Structures*,
Springer Transactions in Civil and Environmental Engineering,
https://doi.org/10.1007/978-981-13-5883-8_23

2010; Millogo et al. 2014; Quagliarini and Lenci 2010) and industrialized fibers such as polypropylene and glass fibers (Balkis 2017; Donkor and Obonyo 2015; Yilmaz 2009).

Among industrialized fibers, the use of polypropylene fibers as reinforcement of earthen materials has been mechanically characterized and results are promising. Yilmaz (2009) assessed the compression and split tensile performance of sand-clay mixtures reinforced with different dosages of micro-polypropylene (MPP) fibers finding that the addition of MPP fibers had a limited effect in terms of the final strength characteristics, but MPP fibers increased the span length of the peak deviator stress. Donkor and Obonyo (2015) studied the effect of macro-polypropylene fibers on the flexural and compressive strength and deformability of stabilized earth blocks finding that flexural strength and post crack performance were improved by the addition of fibers. Balkis (2017) evaluated the effect of waste marble dust and MPP fibers on the compressive and flexural strength of gypsum stabilized earthen materials finding optimum combinations of marble dust and MPP fibers where both compressive and flexural strengths are improved compared to plain gypsum stabilized earthen materials. Although these studies have contributed significantly to the investigation and improvement of polypropylene fiber-reinforced earthen materials, there are still some properties such as impact strength and drying shrinkage cracking of MPP fiber-reinforced earthen materials that have not been explored thoroughly.

The novelty of this research resides in addressing some of the relevant benefits that have not been studied exhaustively such as drying shrinkage cracking control and impact strength increment of adding MPP fibers to earthen materials. Moreover, this study introduces two simple experimental procedures to assess distributed and concentrated drying shrinkage cracking reduction generated by fiber reinforcement of earthen materials. Since earthen material is a generic term, this study refers to the mix between clayey soil, water and fibers as adobe mix since it might be used to produce adobe bricks. The objectives of this study are to evaluate the impacts of different dosages of MPP fibers on: (i) the drying shrinkage cracking performance of adobe mixes; and (ii) the impact strength of adobe mixes.

23.2 Materials and Methods

23.2.1 Materials

The soil used for this study was obtained from southern Santiago, Chile. This soil has been previously used and characterized by Araya-Letelier et al. (2018), obtaining a particle size distribution with a content of 11, 69, and 20% of clay, silt, and sand, respectively. Atterberg liquid and plastic limits were also studied, as well as the plasticity index and specific gravity of solids, obtaining a 29.1, 17.4, 11.7, and 2.51%, respectively. Specific gravity of the soil was determined following ASTM D854 (2000).

Table 23.1 Main properties of micro-polypropylene fibers

Length (mm)	Diameter (mm)	Aspect ratio	Specific gravity (20 °C) (g/cm^3)	Elongation at break (%)	Tensile strength (MPa)
12	0.031	387	1.16	60–140	310

Table 23.2 Adobe mix ID number and material proportion

Adobe mix ID	Oven-dry soil (kg)	Water (kg)	MPP fiber (%)	MPP fiber (kg)
0	1,000	307	0	0
0.25	1,000	307	0.25	2.5
0.5	1,000	307	0.5	5
1	1,000	307	1	10

Commercially available "Sika® Fiber P-12" micro-synthetic polypropylene fibers are used in this study. These MPP fibers are used in concrete and mortar to reduce plastic shrinkage cracking and spalling and to improve impact strength and abrasion resistance. The main MPP fibers' properties are given in Table 23.1.

23.2.2 Adobe Mix Proportions and Specimen Preparation

The workability of the adobe was assessed by hand mixing oven-dry clayey soil with portions of potable water until a homogeneous mix was obtained. The weight of water divided by the weight of the oven-dry clayey soil was defined as the water to soil ratio, choosing a value of 0.307.

This study used four different adobe mixes: a plain mix, and three mixes incorporating MPP fibers (0.25, 0.5, and 1% by weight of oven-dry clayey soil), where the fiber-reinforced adobe mixes were compared with that of plain adobe mix. Table 23.2 shows the adobe mix identification (ID) numbers (where the number indicates the dosage, in percentage, of MPP fibers) and the material proportions for each adobe mix.

To mimic real-life adobe manufacturing, the mixture of the materials, as well as the casting of the specimens, was executed manually. To prevent cluster formation, the MPP fibers were gradually added to the soil and mixed, prior to the water incorporation. Following the inclusion of MPP fibers, water was incorporated in four steps, and the mix was carefully homogenized before each step. The preparation of the different adobe mixes was performed in parallel, covering for two hours each one, after the mixing was finished, to promote material uniformity and equal water absorption. Table 23.3 indicates the different specimens cast for each adobe mix.

The casting of the RILEM beam specimens (i), and slab specimens (iii) was carried out in consecutive layers of approximately 20–30 mm, and each layer was compacted

Table 23.3 Types of specimens cast in this study

Specimen's name	Dimensions (mm)	Test	
		Type	Number of specimens per adobe mix
RILEM beam (i)	160 × 40 × 40, with a 5 × 3 notch at midspan	Impact strength at 7 days	3
		Impact strength at 28 days	3
Flat (ii)	180 × 5 (diameter and height)	Restrained drying shrinkage distributed cracking at 7 days	2
Slab (iii)	600 × 600 × 50, with 2 stress raisers	Restrained drying shrinkage concentrated cracking at 24 h	2

with a tamper to reduce the void content of the mixture. The flat specimens (ii) were cast in only one layer. The RILEM beam specimens (i) were demolded 48 h after casting and kept at 22 °C and 45% relative humidity (RH) for 28 days and rotated 90° to the adjacent side every seven days until testing. The RILEM beam specimens (i) were covered with a plastic bag during their first two days after casting to prevent moisture loss. The flat specimens (ii) were kept at 22 °C and 45% RH for seven days, but they were not demolded neither covered with a plastic bag to generate a restrained drying shrinkage condition, and the generated cracks were assessed at seven days after casting. The slab specimens (iii) were kept in their molds and subjected immediately to an accelerated drying shrinkage process discussed in Sect. 2.3 of this paper.

23.2.3 *Experimental Testing*

To quantitatively evaluate drying shrinkage distributed cracking, two flat specimens were cast for each adobe mix and conserved at laboratory environmental conditions (22 °C and 45% RH) for seven days. The cracks were measured using a 20 × 20 mm grid as guide, a crack width comparator, and a caliper as shown in Fig. 23.1, for each specimen. This procedure has been previously implemented by Araya-Letelier et al. (2018). The values calculated were crack width average (CWA), crack width reduction ratio (CWRR) in accordance with Eq. (1), and crack density ratio (CDR) considering the density of the cracked areas with respect to the total area exposed to drying shrinkage.

$$\mathrm{CWRR_{IDx}} = \left(1 - \frac{\mathrm{CWA_{IDx}}}{\mathrm{CWA_{ID0}}}\right) \cdot 100 \quad (1)$$

where $\mathrm{CWRR_{IDx}}$ is the crack width reduction ratio (expressed as percentage) of adobe mix IDx with respect to the adobe mix ID 0, $\mathrm{CWA_{IDx}}$ is the crack width average of adobe mix IDx and $\mathrm{CWA_{ID0}}$ is the crack width average of the adobe mix ID 0.

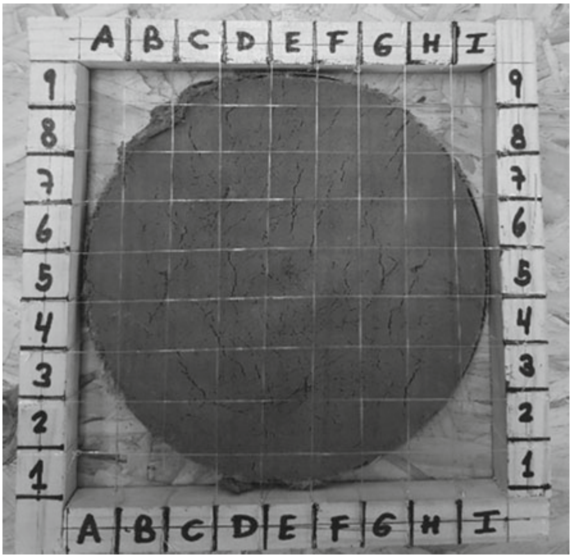

Fig. 23.1 Restrained drying shrinkage distributed cracking procedure

To complement the assessment of the influence of MPP fibers in reducing the restrained drying shrinkage cracking of adobe mixes, a restrained drying shrinkage concentrated cracking test is performed. The slab specimens (iii) were cast into the molds and placed immediately in a room with 42 °C and 20% RH during eight hours and then the specimens were kept at 22 °C and 45% RH for another 16 h. For each specimen, the values of CWA and CWRR were calculated 24 h after casting. The two restrained drying shrinkage cracking procedures presented in this study differ in terms of obtaining a random (distributed) cracking pattern, more representatives of the real working conditions of a material.

The impact strength of each adobe mix was evaluated at seven and 28 days after casting using an approach similar to previous studies (Araya-Letelier et al. 2017a, b, c, 2018), where a sphere projectile is thrown at the center of a specimen, which is supported by a steel frame as shown in Fig. 23.2.

To eliminate damage due to rebound, specimens (i) were attached with silicone to the steel frame, providing also equal support for each one. The total of specimens per adobe mix was six, recording for each one the number of blows required to fracture and collapse it. The total energy at collapse is given by Eq. (2).

$$E_c = n * m * g * h \quad (2)$$

where E_c is the total energy at the collapse, n is the number of blows of the projectile required to collapse the specimen, m is the mass of the projectile (0.047 kg), g is the gravitational constant (9.8 m/s^2), and h is the height of the fall (0.496 m). These

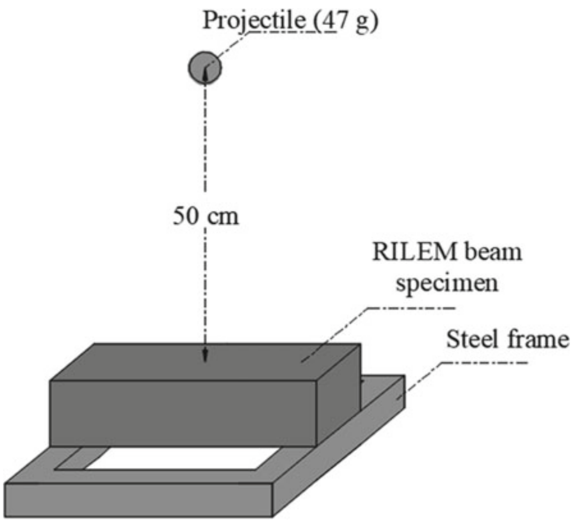

Fig. 23.2 Impact test setup

values were kept constant during the test and, therefore, each blow is equivalent to an impact energy of 0.22 J.

23.3 Results and Discussion

23.3.1 Restrained Drying Shrinkage Distributed Cracking

Figure 23.3 shows one specimen per type of adobe mix at seven days after casting, and it can be seen that a crack width reduction was observed as the MPP fiber dosage increased. Adobe mixes ID 0, ID 0.25, ID 0.5, and ID 1 showed crack widths up to 2.0, 0.85, 0.80, and 0.6 mm, respectively.

The estimated values of CWA and CWRR are shown in Fig. 23.4a in the left and right axis, respectively. It can be seen that values of CWA were reduced and, consequently, the resulting values of CWRR were increased with increasing dosages of MPP fibers. The CWA presented by adobe mix ID 0 (1.1 mm) can be reduced to values that vary between 0.50 mm (ID 0.25) and 0.19 mm (ID 1), which corresponds to CWRR values varying between 54% (ID 0.25) and 82% (ID 1). Overall, as fiber dosage increases the characteristic length between a piece of matrix material and fiber should be statistically reduced and, therefore, there are more chances to have fibers within the bulk that provide crack width control after the matrix develops macroscopic distributed cracks. In addition to reducing the values of CWA and CWRR, the incorporation of MPP fibers also reduces the CDR values as shown in

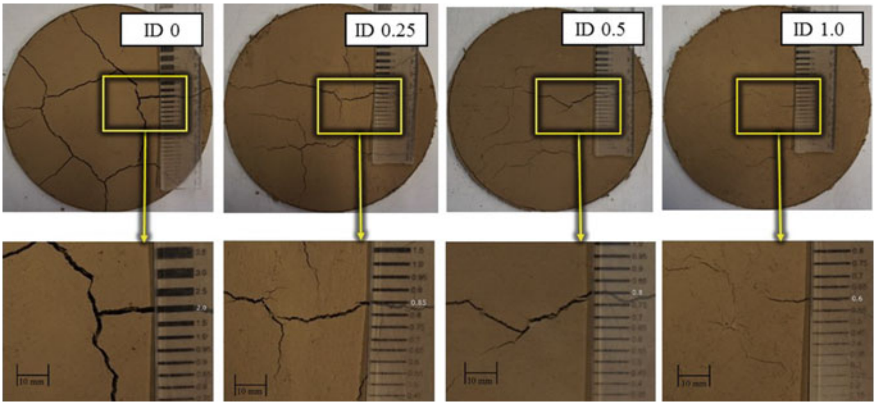

Fig. 23.3 Restrained drying shrinkage distributed cracking results

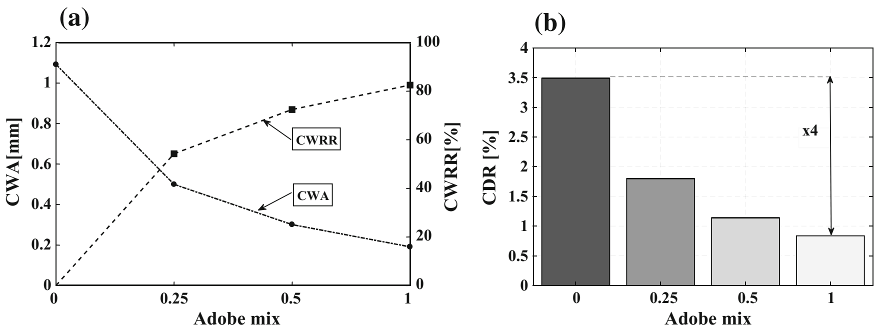

Fig. 23.4 Restrained drying shrinkage distributed cracking: **a** CWA and CWRR results, and **b** CDR results

Fig. 23.4b, where the CDR of the adobe mix ID 0 (3.5%) is four times larger than the CDR value of adobe mix ID 1 (0.84%). Therefore, the incorporation of increasing dosages of MPP fibers reduces both the maximum crack width and the density of cracks due to drying shrinkage when compared to plain adobe.

23.3.2 Restrained Drying Shrinkage Concentrated Cracking

Figure 23.5a presents one cracked slab specimen (iii) per type of adobe mix 24 h after casting and it can be seen that a crack width reduction was observed as the MPP fiber dosage increased. Adobe mixes ID 0, ID 0.25, ID 0.5, and ID 1 showed crack widths up to 6.1, 0.97, 0.88, and 0.71 mm, respectively. The resulting maximum and average crack widths of this test are larger than the corresponding results of the restrained drying shrinkage distributed cracking test for each adobe mix, which

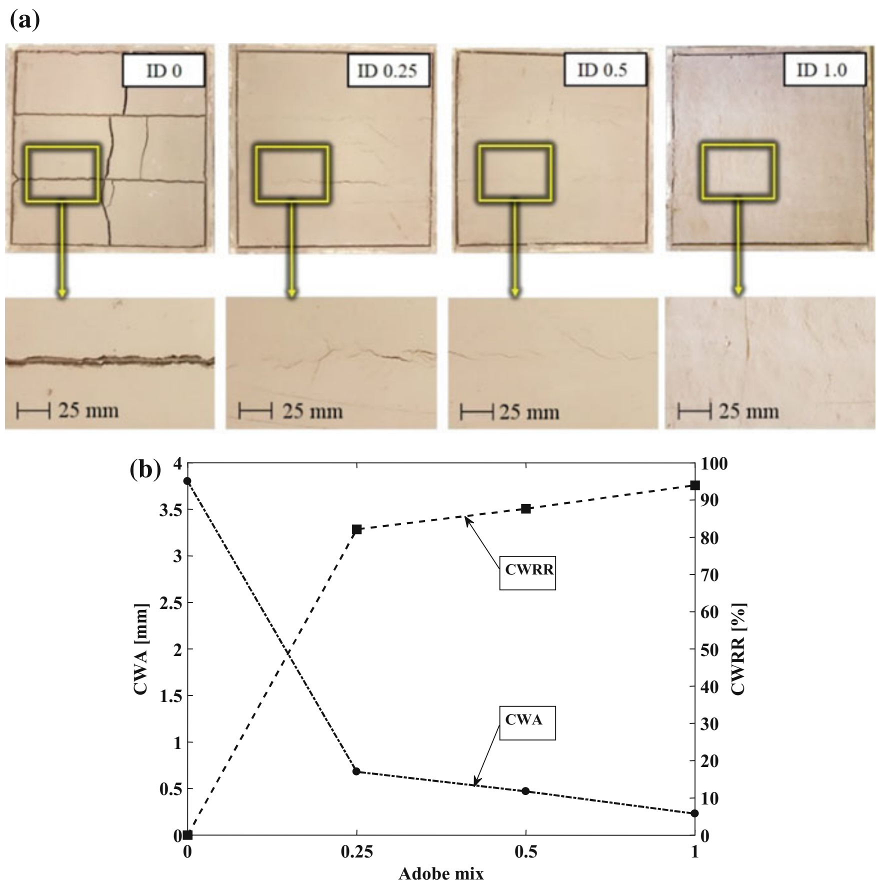

Fig. 23.5 Restrained drying shrinkage concentrated cracking: **a** each adobe mix at 24 h after casting, and **b** CWA and CWRR results

is reasonable due to the use of stress raisers and the exposure to a much more aggressive environmental conditions. However, the increment of the maximum and average crack widths is more significant for adobe mix ID 0 (plain adobe), where the maximum crack width increased from 2.0 mm (distributed cracking test) to 6.1 mm (concentrated cracking test). The MPP fiber-reinforced adobe mixes presented a more thermostable cracking performance compared to plain adobe, where the use of stress raisers and a more aggressive environment in the concentrated cracking test (42 °C and 20% RH) slightly increased the maximum and average crack widths compared to the distributed cracking test (22 °C and 45% RH).

Figure 23.5b shows the estimated values of CWA and CWRR in the left and right axis, respectively, and it can be observed that both, CWA and CWRR, are reduced with increasing dosages of MPP fibers. The CWA presented by adobe mix ID 0

(3.8 mm) can be reduced to values that fluctuate between 0.68 mm (ID 0.25) and 0.23 mm (ID 1), which corresponds to CWRR values oscillating between 82% (ID 0.25) and 94% (ID 1). Overall, as fiber dosage increases the characteristic length between a piece of matrix material and fiber should be statistically reduced and, therefore, there are more chances to fibers within the bulk that provide width control after the matrix develops macroscopic distributed cracks or fibers pullout from the matrix. (Antico et al. 2012; Mindess et al. 2002).

23.3.3 Impact Strength

It is known that manually compacted earthen materials have quasi-brittle behavior (Reman 2004) like other construction materials such as mortars (Araya-Letelier et al. 2017c). In the same way as fiber-reinforced mortars, fiber-reinforced adobe mixes are expected to improve fracture toughness with respect to unreinforced materials and the impact resistance is an effective test to measure the energy-absorbing capacity of fiber-reinforced quasi-brittle materials. At 7 days after casting (Fig. 23.6a), the mean values range from 0.16 (ID 0) to 4.43 J (ID 1), and standard deviation (SD) values range from 0.02 (ID 0) to 1.32 J (ID 1). At 28 after casting (Fig. 23.6b), the mean values range from 0.17 (ID 0) to 13.95 J (ID 1) and SD values range from 0.01 (ID 0) to 3.70 J (ID 1). It can be seen that the impact strength increased as the MPP fiber dosage increased at both ages, but this increment is more significant at 28 days (83 times) than a seven days (28 times). This might be the result of a stronger adobe matrix as well as a stronger bonding between the MPP fibers and the matrix that is developed at later ages. Even the smallest increment in impact energy at collapse, presented by adobe mix ID 0.25, is approximately eight times (at seven days) and 12 times (at 28 days) the required impact energy to collapse adobe mix ID 0. In terms

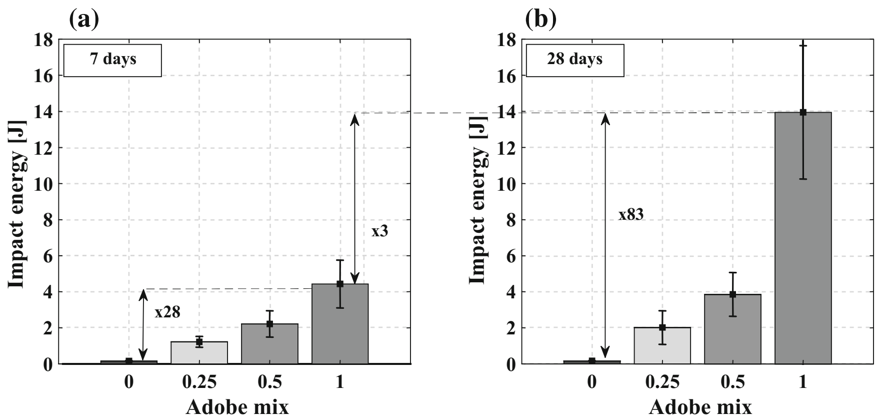

Fig. 23.6 Cumulative collapse impact energy: **a** at 7 days, and **b** at 28 days after casting

of the evolution of impact strength with time, there is a consistent increment from seven to 28 days for each adobe mix, ranging from 7% (ID 0) to 215% (ID 1).

23.4 Conclusions

The drying shrinkage crack widths reduced as fiber dosages increased since more fibers are located in the cross sections that are cracking. The CWRR ranged from 82% (ID 0.25) to 94% (ID 1.0). The CDR values range from 3.5% (ID 0) to 0.84% (ID 1). These results evidence that even small dosages of MPP fibers have a significant impact in mitigating the drying shrinkage cracks in adobe mixes.

The impact strength increased with the incorporation of higher dosages MPP fibers. For adobe mix ID 1 at seven and 28 days after casting, the impact energy at collapse was 28 and 83 times, respectively, to that mix ID 0 (plain adobe). In terms of evolution of impact strength with time, there is a consistent increment from seven to 28 days for each adobe mix, ranging from 7% (ID 0) to 215% (ID 1). This can be attributed to the reduction moisture due to drying.

Acknowledgements The authors would like to thank Arnaldo Puebla, Wladimir Vergara, Mauro Ortiz, Gian Piero Canevari, Matías Riveros, Cristobal Vargas, and Sabine Kunze, for the help provided for the sample preparation, and Sika S.A. Chile, for providing the MPP fibers used in this study.

References

Antico FC, Zavattieri PD, Hector LG Jr, Mance A, Rodgers WR, Okonski DA (2012) Adhesion of nickel–titanium shape memory alloy wires to thermoplastic materials: theory and experiments. Smart Mater Struct 21(3):035022

Araya-Letelier G, Antico FC, Parra P, Carrasco M (2017a) Fiber-reinforced mortar incorporating pig hair. Adv Eng Forum 21:219–225

Araya-Letelier G, Antico FC, Urzua J, Bravo R (2017b) Physical-mechanical characterization of fiber-reinforced mortar incorporating pig hair. In: Proceedings of the 2nd international conference on bio-based building materials and 1st conference on ecological valorisation of granular and fibrous materials. Clermont-Ferrand

Araya-Letelier G, Antico FC, Carrasco M, Rojas P, García-Herrera CM (2017c) Effectiveness of new natural fibers on damage-mechanical performance of mortar. Constr Build Mater 152:672–682

Araya-Letelier G, Concha-Riedel J, Antico FC, Valdés C, Cáceres G (2018) Influence of natural fiber dosage and length on adobe mixes damage-mechanical behavior. Constr Build Mater 174:645–655

ASTM D854 (2000) Standard test methods for specific gravity of soil solids by water pycnometer. ASTM International, West Conshohocken, PA

Avrami EC, Guillaud H, Hardy M (eds) (2008) Terra literature review: an overview of research in earthen architecture conservation. Getty Conservation Institute, Los Angeles

Aymerich F, Fenu L, Meloni P (2012) Effect of reinforcing wool fibres on fracture and energy absorption properties of an earthen material. Constr Build Mater 27(1):66–72

Balkis A (2017) The effects of waste marble dust and polypropylene fiber contents on mechanical properties of gypsum stabilized earthen. Constr Build Mater 134:556–562

Cataldo-Born M, Araya-Letelier G, and Pabón C (2016) Obstacles and motivations for earthbag social housing in Chile: energy, environment, economic and codes implications. Revista de La Construcción 15(3):17–26

Donkor P, Obonyo E (2015) Earthen construction materials: assessing the feasibility of improving strength and deformability of compressed earth blocks using polypropylene fibers. Mater Des 83:813–819

Galán-Marín C, Rivera-Gómez C, Petric-Gray J (2010) Effect of animal fibres reinforcement on stabilized earth mechanical properties. J Biobased Mater Bioenergy 4(2):121–128

Millogo Y, Morel JC, Aubert JE, Ghavami K (2014) Experimental analysis of pressed adobe blocks reinforced with Hibiscus cannabinus fibers. Constr Build Mater 52:71–78

Mindess S, Young JF, and Darwin D (2002) Concrete, 2nd edn. Prentice Hall

Minke G (2000) Earth construction handbook: the building material earth in modern architecture. WIT Press, Southampton

Minke G (2006) Building with Earth: design and technology of a sustainable architecture. Walter de Gruyter

Quagliarini E, Lenci S (2010) The influence of natural stabilizers and natural fibres on the mechanical properties of ancient Roman adobe bricks. J C Herit 11(3):309–314

Reman O (2004) Increasing the strength of soil for adobe construction. Archit Sci Rev 47(4):373–386

Yilmaz Y (2009) Experimental investigation of the strength properties of sand–clay mixtures reinforced with randomly distributed discrete polypropylene fibers. Geosynth Int 16(5):354–363